Use of Integrated Process Rate Analyses to Perform Source Attribution for Primary and Secondary Pollutants in Eulerian Air Quality Models

Harvey Jeffries

Department of Environmental Sciences and Engineering, UNC-CH

Contents

1 Answers to Questions

1.1 Method Overview

1.1.1 Works Only with AQM Models

Integrated Process Rate Analysis (IPRA) or just "process analysis" is a relatively new set of techniques developed at UNC by Jeffries and his students and applied to air quality models (AQMs) as a way to both explain and to understand how the models are producing their predictions. The techniques can be applied to any model that uses "process" descriptions to generate rates of change of state variables in the model and to any state variable that is changed by a series of processes.[1] In AQMs, the processes typically included are emissions of reactive species, horizontal and vertical transport (both advection and diffusion), chemical transformation by gas-phase, liquid-phase, and on particles, deposition to surface, intake and loss through the boundaries of the model domain, and in some cases, nonhydrostatic mass adjustments. The basic operation of these models is to use both "operator-splitting" and a "marching technique" to provide a solution to a governing equation expressing mass balance. In these solution techniques, many of the process changes are computed sequentially for one process at a time over a small time step, h, and the results in the form of a set of "changes" to the state variable[2] are applied to the initial (i.e., at t) condition of the state variable to update it to new conditions at the time $t + h$. Because some process changes are positive and some are negative, *it is impossible to determine how the model produced the final set of state variables by merely examining the beginning and ending state variables* (e.g., the typical concentrations output by the model).

1.1.2 Method Calculates Additional Values in Models

Our basic technique consists of "instrumenting" the model to determine the change caused by each process, and in some cases, performing simple integration of the model's already computed rates over the interval h to convert a rate of change into a concentration change over the interval. We either write these integrated process rate magnitudes out to auxiliary files at frequent intervals, or we use them

[1] The method describes what the model does, not what the atmosphere does. To the extent that the model and the atmosphere are in accord, the method can give insights into how the atmosphere functions.

[2] Usually some form of scaled mass or concentration.

in additional internal model routines we might have added to the basic model code to do on-the-fly processing.

1.1.3 Method Frequently Involves Post-processing of Model Output

Sometimes additional manipulations of the process rates are needed to reveal exactly how the model functions. For example, we output the integrated reaction rate (IRR) of each reaction in the chemical transformation mechanism. By performing additional clustering and cycle analysis on these concentration changes in a reaction merging and tracking technique we call IRR/MB, we can produce more universal and more abstract parameters of chemical mechanism performance. As an example, we routinely determine how many times each hydroxyl radical was being used before being terminated, or what was the average number of nitric oxide oxidations per reacted volitile organic compound (VOC), i.e., the organic reactivity. These can give deep insight into not only the workings of the chemical mechanism itself, but they also reveal the very strong dynamic interaction among the physical (i.e., meteorological) processes in the model and the chemical transformations. By viewing the chemisry at an abstract level of initiation, propagation, and termination, we gain a measure of model performance that is comparible across different chemical mechanisms, operated in different chemical models, on different domains, even at different times of the year.

1.1.4 True Secondary Species Source Attribution

In our most sophicated—and the most computationally demanding—analysis, we produce "process compositions" of various model species, e.g., ozone (O_3), nitric oxide (NO) and nitrogen dioxide (NO_2), the VOCs, and carbon monooxide (CO). By process composition, we mean to state the fraction of the mass or concentration in a model cell or aggregate group of cells in terms of the process that gave rise to this portion of the mass or concentration. (This is source attribution.) The processes that we usually distinguish in the composition are:

- *initially here*—meaning the this mass fraction was present in this cell (or set of cells) at the start of the analysis;
- *initially in other cell*—meaning that this mass fraction was initially in cell *i* at the start of the analysis;

- *boundary (east, west, north, south, aloft)*—meaning that this mass fraction was added to the model analysis domain by inflow at a boundary;
- *emitted here*—meaning that this mass fraction was emitted into this cell at time *t* during the analysis;
- *emitted in other cell*—like initially in other cell, but for emissions;
- *chemistry here*—meaning that this mass fraction was chemical produced in this cell during the analysis period;
- *chemistry in other cell*—meaning that this mass fraction was chemical produced in cell *i* during the analysis period.

Note that transport is not a contributer to the process composition because transport does not create any mass, it just moves it from cell to cell. Also notice that "loss processs" do not appear in the list either as these are not responsible for any of the mass in the cell(s).

The mechanism for accomplishing this compositional analysis (other than the already described IPR output for each analysis cell at each transport time step) are "history lists" that record the previous process compositions in all analysis cell, the magnitude of the cell to cell transfers caused by the transport processes, and the magnitude of new emissions over the step.

When a process composition analysis (PCA) is started, all the masses (concentrations) in the cells of a selected model domain (usually a sub-set of the whole model domain) are considered to be 100% "initially here" composition. By monitoring the horizontal and vertical transport processes computed by the model in a single advective time step, we can compute how much of each cell was moved into adjacent cells and we can know how much of the original mass in the cell was left. By using these to combine information from two or more cell's history lists, we can compute a new process composition in the target cell. Because there is but one concentration of each species in each cell, removal processes apply directly proportional to the process compositions in the source cell. Thus the material leaving a cell has the same process composition as the cell it is leaving. This "bookkeeping" is repeated for all processes and all analysis cells every cycle of the model's evaluation of its processes. Mass that enters cells at the edge of our analysis region or at the edge of the model domian, is labeled as "boundary" process mass regardless of its actual origin.

By combining the PCA chemical composition with the IRR/MB analysis of the chemical transformations in the cell in which the chemistry occurred, we can trace the "source" of a secondary species like O_3 back to its precursors. That is, we can answer questions such as

> "How much of the O_3 in a cell that exceed the standard at a particular time was produced by biogenic isoprene reacting with NO_x emitted by light-duty trucks on a major arterial highway two cells to the east?"

What I have been describing is a "backward" technique based on keeping a history of process composition on a cell by cell basis. Viewing this history list data a different way, we can do a forward analysis and answer questions such as

> "How much O_3 is produced, and in which cells, from the NO_x emitted by a natural gas pumping station located at the edge of the city?"

1.2 Key Assumptions

There are two classes of assumptions: those that arise in "instrumenting" the model and in the subsequent calculations, and those that the model makes about the world, i.e., assumptions made in formulating the model, in producing a model solution, and assumptions in producing the model inputs.

1.2.1 Assumptions in measuring what the model is doing

Attached to the end of this presentation is a section from a paper in preparation that describes the "instrumenting" of the SAQM model. This shows how we split process descriptions included in the model to permit us to find the gain and loss rates of each process or sub-process for each species we are tracking. In addition we describe how the history lists are updated in exactly the same order as the model computed the changes it applied to the concentrations at the end of the time step.

In some cases,we perform a simple first-order integration of a process rate over the interval h, where we know the model's computed rate at t and at $t + h$. We typically use the average of the rate in a simple trapezoidal rule calculation to integrate the concentration change caused by this process over the interval. This results in small errors compared to the model's usually integrator. The effect of these errors is that there is not quite a mass balance of all processes over the time step. These mass balance errors rarely exceed a few 0.1's of ppbs.

1.2.2 Assumptions in model formulation, solution, and inputs

Our method merely reports on what the model is predicting. To apply its results in the real world requires that one have faith that the model was an accurate representation of the world's events. We are in no worse a position than the regulator who wants to use the model to predict the control requirements needed to meet a standard, and in some senses we are in a better position. This is because we can at least explain how the model made its predictions and we examine that each of the process changes, by itself, appears reasonable.

1.3 Limitations

Out analysis is limited to those situations in which there is an acceptable AQM simulation on a machine with sufficient RAM and disk storage that can accomidate the increases in runtime storage and file output needed by the IPRA method.

A major limitation is that the AQM's computer code must be changed to compute and output the IPR data. This has prevented us, for example, from inserting our codes into the UAM-V AQM, and thus prevented us from performing any OTAG process analysis.

A second, but transient, limitation is the qualty, robustness, and user friendlyness of the current post processor codes which are all student-quality codes.

The various types of analysis are at present require a fair level of routine file manipulation to produce the interpertable output.

Increasingly, computer storage, both at runtime and for the files is becoming less and less of a limitation year by year.

1.4 Required Data Bases

Whatever the model requires. We also need an accurate listing of the AQM's chemical reaction mechanism in the exact order used by the AQM.

When problems are found in the model's performance, we need access to the files used to prepare the model's inputs and we need to understand the assumptions that went into these. Sometimes this need extends to very fine detail in the model preperation inputs, such as particular VOC speciation profiles (see the example described below).

1.5 Computational Requirements

The additional computational load for standard IPR data output can hardly be detected, except for the additional I/O time. Several species and reaction vectors must be added to the AQM which increase their runtime storage needs. For desirable size analysis domains, the total output file sizes can double the size of those for a non-IPR-data producing run.

The PCA storage and computational load are currently comparable to the AQM itself. This is in part the result of poor algorithms and internal storage organization, and these can be dramatically reduced by a re-write of the program.

The Contineous PCA implemented in the SAQM code, adds 2500 storage locations per cell being tracked. This method permits the top 100 contributers for each of five processes (initial, boundary, emissions, chemistry, and nonhydrostatic mass adjustment) to be tracked for five principle species (O_3, NO, NO_2, CO, and VOC) within a cubic area of the modeling domain. The tracking domain is limited by the available RAM on the executing machine. We have a 2-gigabyte RAM UNIX workstation available to us for this program which will permit at least a 25 by 25 by 10 level analysis domain.

1.6 Expertise Required

Significant expertise is required to insert the "instrumenting" code into the AQMs. Once this is done, however, anyone who can run the AQM, can readily produce IPR-data files.

The more simpler types of IPR-analysis, such as the process time series plots, are quite simple to produce and anyone who knows how to do routine file manipulations and can execute model programs can produce the IPR time series graphs. Recent changes in the IRR/MB program and the creation of two Microsoft Excel spreadsheets, have also automated the production of the set of nine chemistry tables and the two main chemistry cycle diagrams, as well as producing pie charts of radical sources and O_3 produced by each VOC.

Once the tables and figures are produced, interpretation of results requires a good understanding of urban atmospheric chemistry and requires some training using various examples of IPRA.

1.7 Method Documentation

Within the last four years, a book chapter [1], five journal articles [2–4, 7, 8], two additional manuscripts [5, 6], two national AWMA meeting presentation papers [9, 10], two Ph.D. thesis, a M.S., a 142-page research report to the Gas Research Institute giving detail applications examples [12], and a memo report on the results of a SIP application analysis [11] have been published. Electronic preprints (i.e., PDF-files) of many of these can be obtained over the Internet at
`ftp://airsite.unc.edu/pdfs/ese_unc/jeffries/ipradocs/`.

There is a User's Guide on the IPRA inputs and controls for both the UAM-IV and the UAM-V.

A modified version of the UAM-IV with IPRA output is available via the internet, along with the IRR/MB codes and the spreadsheets. These have all been provided to a number of contractors, researchers, and state agencies.

Currently we are installing IPRA code into the version of SAQM that is publically distributed by the California Air Resources Board under a contract to CARB.

1.8 Output Produced

Outputs are in the form of time series plots of process magnitudes and species concentrations, chemical cycle diagrams, pie charts of distributions of important chemical parameters, and tables giving supporting details should questions arise from examining the plots and diagrams.

For PCA, outputs are time series area plots of species' concentration and process composition.

1.9 Complementary Analysis

Our results are best compared with ambient observations that can be used to derive a "process rate." We are working with Robin Dennis at EPA/NOAA to generate a "process evaluation" approach for model testing.

1.10 Uncertainty Associated with Estimates

Our answers are as uncertain as the model is.

1.11 Performance Evaluation

In one sense, IPRA, is an evaluation of the model's performance in that we constantly check for mass balance over all the model's processes and solution methods. (See example below where we find an NOx mass imbalance in UAM-IV).

1.12 External Review

The fundamental principles of IPRA have been published in peer-reviewed journal articles and the PCA applications have been presented in public forums and analyses have been presented to private and state AQ officals.

1.13 Portability

Model code changes are in the base language of the model. We have made code changes on CRAYs and various UNIX workstations.

Some of the post processing programs are in FORTRAN and some are in C++. C++ is available on essentially all workstations and on the CRAY.

1.14 Future Work

Dr. Tonnesen is working at EPA/NOAA installing various IPR analysis tools in to the HRADM used by Robin Dennis to perform model-based research. This includes using IPRA to explain the results of "source modulation" model experiments.

Dr. Tonnesen and Mr. Gerald Gipson (Jeffries's PhD student) are installing IPRA into the MODELS3 framework.

Under CARB funding, Jeffries and his students will continue to install IPRA codes into the SAQM and will perform demonstration analyses for the SARMAP simulations.

Work needed includes a complete re-write of the IRR/MB program to make it more efficient, and easier to operate as a graphical interface, "clickable" post processor to produce visualizations of various processes from a simulation.

The PCA algorithms used by Lo need to be significantly restructored to reduce both memory and computational time.

A unified file format for IPRA data that is more platform independent and that meets the needs of all the post-processing programs in a more efficient manner is needed.

A most pressing need is to conduct many more IRR/MB and PCA analyses of various scenarios to prepare a much better training set and to use these to prepare guidance documents on how to apply IPRA for model evaluation and source attribution.

2 What is “Source Attribution”?

In the bottom two kilometers of the atmosphere, ozone (O_3) mixing ratios above a range of 40–70 ppb are almost always produced in by photochemical reactions in the lower atmosphere.

In the simplest explanation that can be given, such ground-level O_3 comes from reactions of oxides of nitrogen (NO_x), so that in the absence of NO_x there can be no O_3 production (except for electrical discharge). Unfortuately, availability of NO_x is a necessary but not sufficient condition for O_3 creation or “sourcing”. The other necessary ingredients are a source of inorganic and organic peroxy radicals, $HO_2^{\cdot}$ and $RO_2^{\cdot}$, which are formed mostly from radical attack on VOCs. It is the reaction of these $RO_2^{\cdot}$ radicals with NO that “splits” the molecular O_2 bond, and produces an “odd-oxygen” atom, which is initially attached to the nitrogen in NO_2. Photolysis of NO_2 frees this “odd-oxygen” to react with O_2 to make O_3.

So the task of explaining the source of O_3 becomes the task of explaining the source of the NO_x that was used by the peroxy radicals to make O_3, and explaining the origins of the $HO_2^{\cdot}$ and $RO_2^{\cdot}$ radicals that picked up the oxygen that would eventually make O_3.

The peroxy radicals are made mostly by hydroxyl radical ($^{\cdot}OH$) attack on VOCs, so explaining the peroxy radical’s origins means explaining the $^{\cdot}OH$ radical’s origin.

It turns out that in most AQMs, more than half of all the $^{\cdot}OH$ that reacts in the model, came from O_3 photolysis! That is because, due to VOC oxidation being a chain process, each $^{\cdot}OH$ that initially attacks can be recreated to attack again, and again. . . up to 5–6 times. With sufficient NO_x each $^{\cdot}OH$ radical can make 4–5 O_3 molecules, some of which photolyze to make $^{\cdot}OH$.

Many of us who have been studying this problem now actually study the source of all “odd-oxygen”, which is the necessary step if O_3 is going to be produced. The “odd-oxygen” can reside on a number of carriers, one of which happens to be O_3. Thus, the source of O_3 is really an odd-oxygen production problem, followed by an odd-oxygen species partitioning problem.

It turns out that it is fairly easy in a model to measure the spatial and temporal distribution of odd-oxygen *production*. It is also fairly easy to track the transport of odd-oxygen. But predicting its partitioning among the variety of odd-oxygen carrying species is much more difficult.

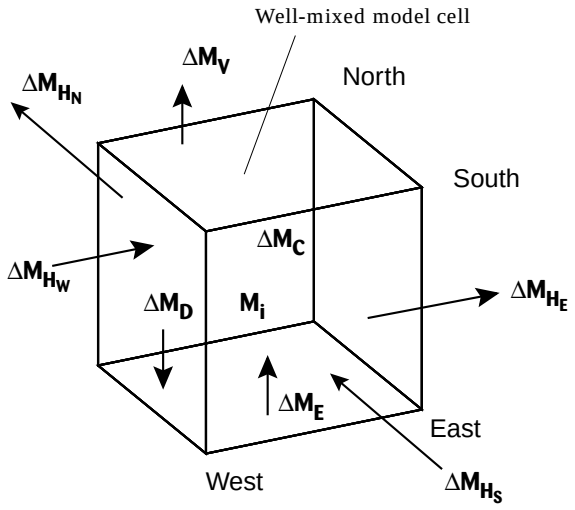

H is horizontal transport
V is vertical transport
E is emissions
D is surface deposition
C is chemical transformations
i is initial
f is final
M is species mixing ratios

$$\Delta M_H = \Delta M_{H_N} + \Delta M_{H_S} + \Delta M_{H_E} + \Delta M_{H_W} \quad \text{net horizontal change}$$

$$\Delta M_V = \Delta M_{V_u} + \Delta M_{V_d} \quad \text{net vertical change}$$

$$M_f = M_i + \Delta M_H + \Delta M_V + \Delta M_E + \Delta M_D + \Delta M_C \quad \text{total mass balance}$$

Figure 1: Processes operating on a cell in an air quality models.

2.1 What is Process Analysis?

2.1.1 The Model Processes

Most air quality models create output files of just species concentrations over space and time. In "process analysis" we focus on the change caused by each major physical and chemical process in the model (see Figure 1), and thus our method requires additional model outputs. The processes that we need separately quantified *at each time step* are:

Chemistry: To perform a complete system analysis of the chemical transformations, the integrated reaction rates, or IRRs, of each chemical reaction in the model are needed. The reaction rate and IRR for a second order reaction is defined as

$$\begin{aligned} r_g &= k_g M_i M_j \\ \Delta r_g &= \int_{t_1}^{t_2} r_g \mathrm{d}\, t \end{aligned}$$

where M_i and M_j are the mixing ratios of reactants in reaction g, and k_g is the reaction rate constant. In addition for other types of process analysis, we need the

net change in each species' mixing ratio caused just by the chemistry, ΔM_C. This value and other similar values are obtained by integrating the rate of change of each process separately rather than summing all rates of change and then integrating once, that is,

$$\Delta M_p = \int_{t_1}^{t_2} \frac{\mathrm{d}\, M}{\mathrm{d}\, t}\Big|_p \mathrm{d}\, t$$

and p indicates the process.

Horizontal transport: The change in each species' mixing ratio caused by advection, ΔM_H, from cell to cell by winds must be quantified and

$$\Delta M_H = \Delta M_{H_N} + \Delta M_{H_E} + \Delta M_{H_S} + \Delta M_{H_W}$$

where the subsubscripts indicate the direction of transport from the north, east, south, or west into the cell.

Vertical transport: The change in each species caused by advection and diffusion of material, ΔM_V, from above and below each cell must be quantified.

Emissions: The change in each species caused by emissions, ΔM_E, into each cell must be quantified. It is also useful to distinguish low level emissions from elevated emissions.

Deposition: The change in each species caused by deposition of material on surfaces, ΔM_D, must be quantified.

Initial: The concentration of each species at the beginning of the time step, M_i, is also needed, i.e., the initial species concentrations for the time step.

It is clear that

$$M_f = M_i + \Delta M_C + \Delta M_H + \Delta M_V + \Delta M_E + \Delta M_D$$

where M_f is the final concentration for each time step. Obviously, some of the terms on the right-hand-side will be negative and some will be positive, so at any given time different processes are driving the species' mixing ratios up and some are driving it down. In an analysis of mixing ratio predictions, it is not possible to explain the mixing ratio time series by just examining the mixing ratios. Therefore,

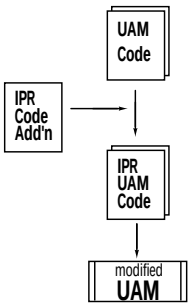

Figure 2: Air Quality Models must be modified to include new code to output the process rates.

in the IPRA method, all of the additional output described above is subjected to further processing by several auxiliary or post-simulation programs. The code changes needed and the auxiliary programs will be briefly described next.

2.1.2 The Code Changes

To perform process analysis, minor additions (less than 500 lines) must be made to the solver codes in each air quality model to be analyzed and a new executable version of the model must be produced (see Figure 2). These changes have already been made to the regulatory version and to our CRAY vectorized version of UAM-IV, to the High Resolution RADM, and are currently being made to the UAM-V. In making these changes, a small amount of additional code is added at the end of each of the process routines in the model [13]. The purpose of this new code is to perform a *simple* integration of the rate of each process that effects species concentrations over each model solution time step and, depending upon a user command, to either accumulate these integrated rates for an hour before writing them out, or to write them out each time step. Thus the model’s output will consist of both the usual species concentration data and the new IPR data (see Figure 3). These additional model calculations use the *process rates of change* that the model already computes and thus place only a very small additional computational burden on the system. An abbreviated example of the extract of one time step output from an IPR file is shown in Tables 1 and 2.

For an environmental chamber analysis or for a Lagrangian air quality model analysis, the total output file consists of a set of values like those in Tables 1 and 2, usually one set for each hour. Note that some of the items in the IPR file are not needed for these simple types of analysis, e.g, the horizontal transport terms, and in these cases these items are written out as a field of zeros. In other cases, some

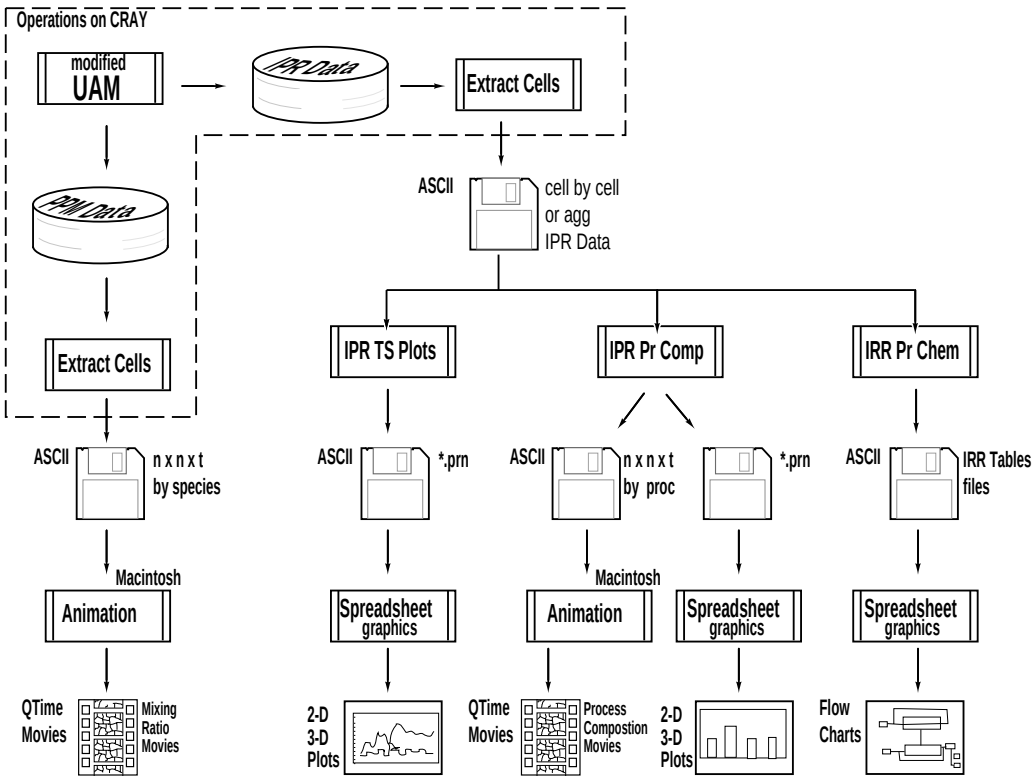

Figure 3: Schematic of a ‘complete’ process analysis for a model scenario run

species are computed by a steady-state approximation and are not transported from cell to cell. These species therefore appear with small initial values and have zero rates for many physical processes. For an Eulerian model, such a set as in the tables would be written for each cell of the model, resulting in a large amount of additional output–nearly a doubling the output of the model if all cells are written out. For this reason, the changes made to the UAM allow rectangular “regions” to be selected for process analysis output. Furthermore, some types of process analysis (e.g, the process compositional analyses) require output data at every advective time step (6 minutes for the UAM), while the rest use values accumulated for one hour.

For efficiency in storage and for speed during the simulation, the IPR data are written as binary data in a model-specific format. At the present time, a post-simulation program EXTRACT is used to select cells and times from the binary file and to produce ASCII files that are portable to other computing platforms such as PCs. While the hourly output for 0500–1900 LDT for a single cell in the ASCII format is only 152 kilobytes, the “every-time-step” output needed for

Table 1:. The first part of the Integrated Process Rate output: the integrated reaction rates of each chemical reaction in the model for one time step.

```
"IR/MB FOR UAM-IV"
Time =    11. Dark =    F
!"Rxn no      Int rate"
{  1}      1.28502E-01
{  2}      3.08729E-01
{  3}      1.06341E-01
{  4}      3.61750E-06
{  5}      6.07917E-07
{  6}      1.33169E-07
{  7}      9.16786E-04
{  8}      1.71110E-01
{  9}      1.02786E-02
{ 10}      8.84278E-03
  .         . . . .
{ 24}      1.60628E-05
{ 25}      1.61543E-12
  .         . . . .
{ 81}      4.34745E-04
{ 82}      0.00000E+00
{ 83}      0.00000E+00
{ 84}      2.74100E-06
{ 85}      9.53471E-05
{ 86}      0.00000E+00
;
```

Table 2:. The second part of the Integrated Process Rate output: the integrated process rates of each physical and chemical process in the model for one time step.

```
! Species      Init conc        Gas Chem         West Trans       East Trans       South Trans      North Trans
"O       "     0.100000E-19     0.000000E+00     0.000000E+00     0.000000E+00     0.000000E+00     0.000000E+00
"O1D     "     0.100000E-19     0.000000E+00     0.000000E+00     0.000000E+00     0.000000E+00     0.000000E+00
  .                 .                .                .                .                .                .
"PAR     "     0.604878E-01    -0.561872E-02     0.445677E-01    -0.473587E-01     0.487423E-03     0.636204E-02
"TOL     "     0.127839E-02    -0.387130E-03     0.839104E-03    -0.936106E-03     0.102265E-04     0.103055E-03
  .                 .                .                .                .                .                .
"ISOP    "     0.176950E-04    -0.242456E-03     0.340836E-04    -0.370586E-04     0.930889E-07     0.382198E-05
"CLBR    "     0.993197E+00     0.000000E+00     0.823980E+00    -0.829784E+00     0.868804E-02     0.115545E+00
;

! Species      Titrate          Ver Trans        Low lev emis     Elev PT emis     Deposition       Final conc
"O       "     0.000000E+00     0.000000E+00     0.000000E+00     0.000000E+00     0.000000E+00     0.100000E-19
"O1D     "     0.000000E+00     0.000000E+00     0.000000E+00     0.000000E+00     0.000000E+00     0.100000E-19
  .                 .                .                .                .                .                .
"PAR     "     0.000000E+00    -0.150652E-01     0.699708E-02     0.101726E-04     0.290276E-14     0.508696E-01
"TOL     "     0.000000E+00    -0.409817E-03     0.324779E-03     0.000000E+00     0.551037E-16     0.822499E-03
  .                 .                .                .                .                .                .
"ISOP    "     0.000000E+00    -0.543736E-04     0.304680E-03     0.000000E+00     0.147928E-17     0.264846E-04
"CLBR    "     0.000000E+00    -0.113493E+00     0.000000E+00     0.000000E+00     0.515579E-13     0.998133E+00
;
```

the process compositional analysis is 1.8 megabytes per cell for the same time period, and typically a 25 by 25 cell region is analyzed resulting in having to transfer and store 65 megabytes of data. We are therefore considering changing the EXTRACT program to output HDF data sets as an alternative to the ASCII format. HDF, or hierarchal data format, was invented at the National Center for Supercomputing Applications for exchanging data among different applications. It can also exchange binary data among different computer platforms, e.g., CRAY’s and PC’s. HDF will be described in more detail later.

2.1.3 The Process Analyses

As shown in Figure 3, presently there are four basic types of process analyses:

1. *Movies of lumped process magnitude fields*, i.e., show by color in each model cell, for each hour, the total new radical production, and in another movie the odd-oxygen production, and in a third movie the total termination product formation (i.e., the beginning, middle, and end of the chemical cycles) and *movies of species concentration fields*, e.g., movies of O_3, O_x, NO, NO_2, CO, and VOC mixing ratios in each cell each hour. These movies are useful combined in a spatial and temporal analysis. These will not be described any further.

2. IPRA *time series* plots that show a time series of the mixing ratio of selected species (e.g., NO, NO_2, O_3, CO, and total VOC) along with the time series of the change produced each hour by chemistry, net horizontal transport, net vertical transport, elevated and low level emissions, and deposition. These plots have been typically produced by common PC spreadsheet programs using `ASCII` text files that are imported into the spreadsheet program.

3. IPRA *process composition* plots and movies. In this analysis, the composition of a selected species in a given cell at a particular time is expressed in terms of the following sources:

   (a) *initial-here*–the fraction or mixing ratio that was initially present in the target cell (and still remains);

   (b) *initial-other*—the fraction or mixing ratio that was initially present in some other cell and was subsequently transported to the target cell;

   (c) *emitted-here*—the fraction or mixing ratio that was emitted into the target cell (and still remains);

   (d) *emitted-other*—the fraction or mixing ratio that was emitted into some other cell and was subsequently transported to the target cell;

   (e) *chemistry-here*—the fraction or mixing ratio that was chemically formed in the target cell (and still remains);

   (f) *chemistry-other*—the fraction or mixing ratio that was chemically formed in some other cell and was subsequently transported to the target cell;

   (g) *boundary-horizontal*—the fraction or mixing ratio that was transport through a N, S, E, or W domain boundary face and was subsequently transported to the target cell;

(h) *boundary-vertical*—the fraction or mixing ratio that was transported through a top or bottom boundary face and was subsequently transported to the target cell.

The simplest form of this output is an area chart for the composition in the target cell over time. Movies, one for each process (i.e., initial, emission, chemistry, vertical boundary, and horizontal boundary), that show the spatial and temporal distribution of the process contribution to a selected target cell are the most complex form of output for this analysis. Note that it is possible to reverse this analysis and report the contribution of a particular source to all affected cells. The data processing for this analysis has typically occurred on large memory PCs with visualization via PC spreadsheet tools.

4. *Integrated Reaction Rate or* IRR/MB *process analysis* is applied to just the chemical transformation change. It is usually presented in the form of time series, piecharts, flowcharts, and systems diagrams. These outputs include:

   (a) time series of new radical strength and pie charts of source composition;

   (b) time series and average hydroxyl radical chain length, or number of times each hydroxyl radical is used before being lost; time series and average NO chain length, or number of times each NO is oxidized to NO_2 before being lost as a nitrogen product;

   (c) the amount of VOC consumed by hydoxyl radicals, by O_3, or by photolysis reactions, and the average number of NO-to-NO_2 conversions per VOC reacted;

   (d) the amount of O_3 produced by each VOC reacted;

   (e) the total odd-oxygen production, the average O_3 yield per NO_2 photolysis, and the total amount of O_3 produced;

   (f) the VOC and NO_x propagation factors and the distribution of termination products;

   (g) the amount of O_x and O_3 formed by each VOC in the system;

   (h) detailed VOC and nitrogen mass balances.

   The data processing for this analysis has typically occurred on PCs or VAXes and results in collection of 12 ASCII tables being produced. Selected data from these tables are manually entered into spreadsheets or onto plots produced via PC/Mac Drawing programs.

Examples output from some of these analyses will be briefly described below.

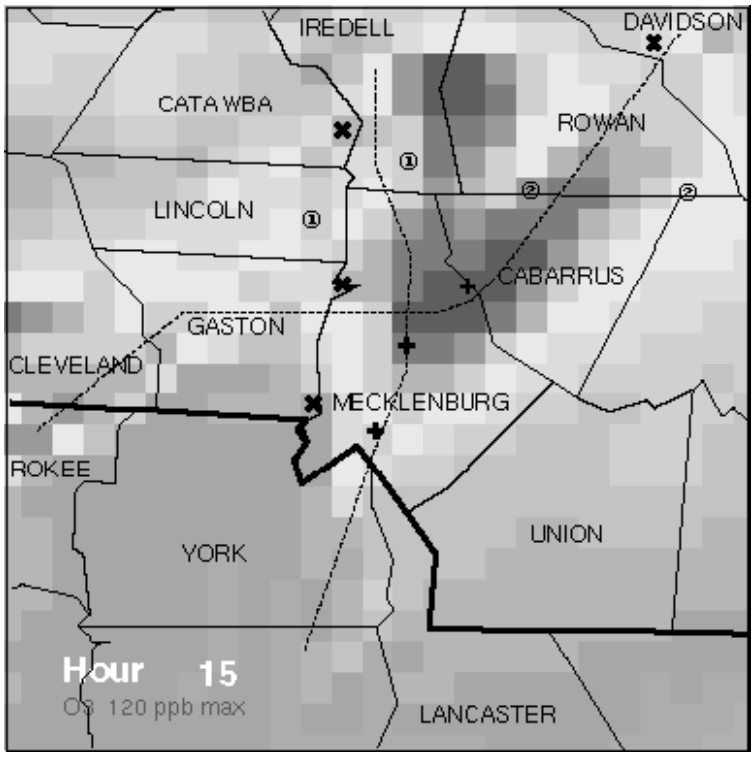

Figure 4:. One frame from day two of a UAM movie of ozone mixing ratios for a 1988 Charlotte, NC episode. The darkness is not proportional to O_3 in this figure and both deep blue (for no O_3) and bright red (for O_3 equal to or exceeding 120 ppb) both show as dark colors.

2.2 Example Analyses Results

The purpose of this section is to demonstrate what some of these process analyses look like. This work, conducted as part of our work on a EPA cooperative agreement, work with the NC Department of Environment, Health, and Natural Resources on the state’s request for re-designation for Charlotte NC, work for a DOE project, and work on a GRI contract has for the most part occurred recently and thus has not yet reached the literature.

2.2.1 Movies of Concentrations

The movies have one frame for each hour of a 24-hour simulation and play in 24 seconds. Often of more value is the ability to stop the movie play and “rock back and forth” over a series of frames to gain insight into what changed over the time interval. Figure 4 is a grayscale rendition of one frame from the O_3 mixing ratio

movie for day two of a 1988 Charlotte, NC episode basecase simulation. While the color transformations to grayscale are not linear, this frame still shows the essential features of the UAM movies:

- ❏ the total view is 25 by 25 cells centered on downtown Charlotte;
- ❏ the cell size is 5 by 5 kilometers and is clearly visible in the figure;
- ❏ county lines are marked in black and the NC-SC state line is marked in bold black;
- ❏ the dotted lines are the approximate locations of two Interstate highways; the one that runs diagonal is I85 and the one that runs N-S is I77;
- ❏ the legend for map symbols is:
  - ◆ the three ✚-marks are the sites of the monitoring stations in Charlotte (S to N, Arrowwood, Plaza, and County line);
  - ◆ the four ✖-marks are the sites of Duke Power's fossil fuel power plants;
  - ◆ the ①-mark in Lincoln county is the future site of Duke Power's gas turbine station for meeting peak power demand (this was not present in the 1988 base case, but was in the future 1999 and 2005 cases);
  - ◆ the ①-mark in Iredell county is a natural gas pumping station;
  - ◆ the ②-marks are smaller low level NO_x sources.

By comparing the movie frames of species mixing ratios, e.g., O_3, with movie frames of lumped processes such as total odd oxygen production per hour per cell, one can see spatial and temporal relationships that would be difficult to achieve any other way. For example, by showing total odd oxygen production locations a few hours before the peak O_3 time, we can determine the most important sources that should be controlled to reduce the O_3 maximum. Comparisons of frames from process composition movies to be described below with the usual species mixing ratio movies also helps gain insight into complex spatial relationships.

2.2.2 IPRA Time Series

Figure 5 shows process analysis time series plots for NO, NO_2, VOC, and O_3 for a Charlotte UAM scenario in 1987. These are probably the outputs that are the most useful to non-modelers, as the concept seems so obvious to most. In this example, the IPR data values were aggregated for a 6×6 cell region that included both the Arrowwood and Plaza monitors for this analysis. The 1987 episode was very stagnant and the UAM was having problems predicting accurate O_3 mixing ratios in areas south of the center city, e.g., see the large *late* increase in O_3 in Figure 5. The measured peak maximum for this day was 131 ppb (see Fig. 7)

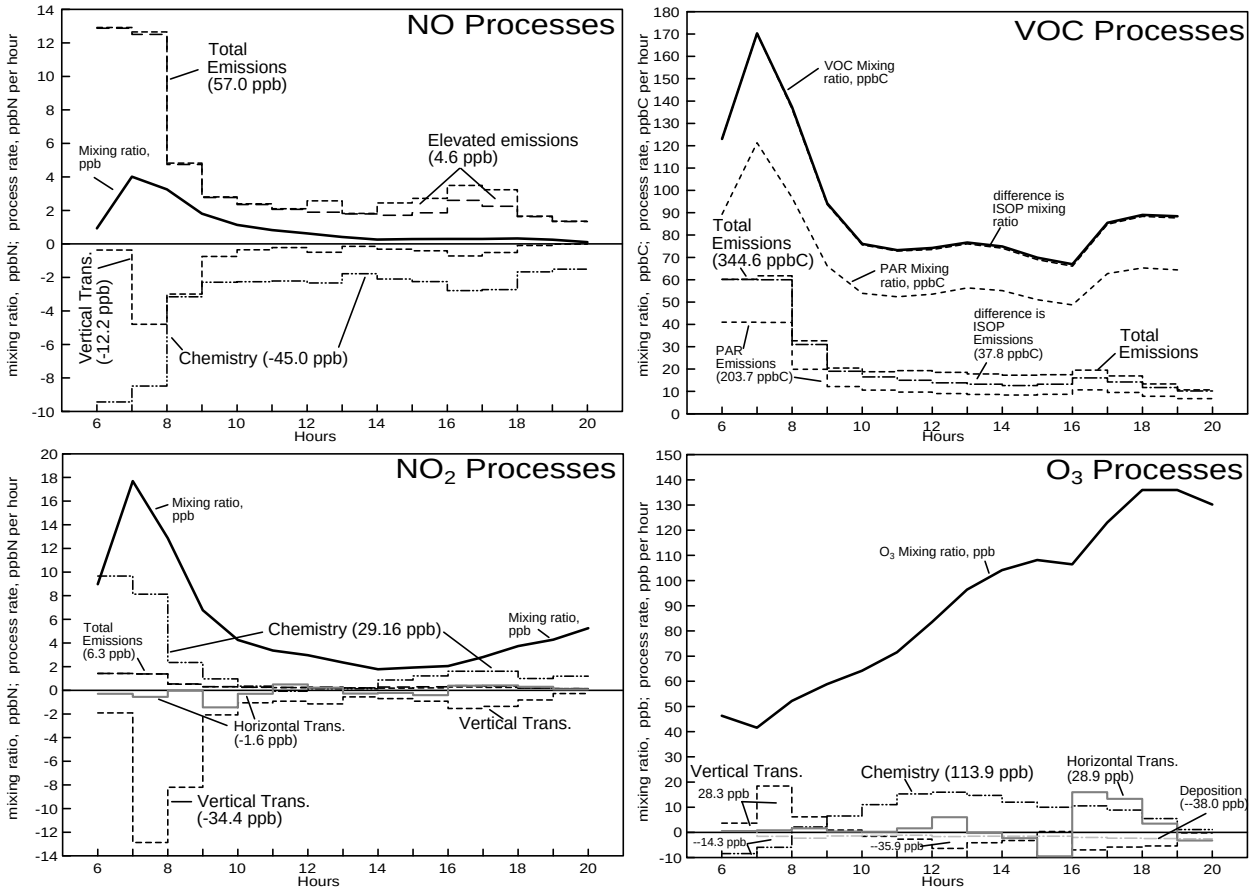

Figure 5: Process time series for Charlotte 1987 episode.

Nitric Oxide: In the NO processes plot, we see that emissions in the 6×6 area increased the NO mixing ratio by 57 ppb over the time period 500–1900 LDT and only 4.6 ppb came from elevated sources. Chemistry process were the major consumer of NO, removing 45 ppb NO over the day. Vertical transport was an important process for NO in the morning hours, but decreased to small values during the afternoon when the NO mixing ratio was being driven to low values by the chemistry processes.

Nitrogen Dioxide: In the NO_2 processes plot, we see that NO_2 emissions were a much smaller contributor to NO_x, only 6.3 ppb. Chemistry contributed the large majority of the NO_2, 29.6 ppb, but note that the increase in NO_2 was less than the

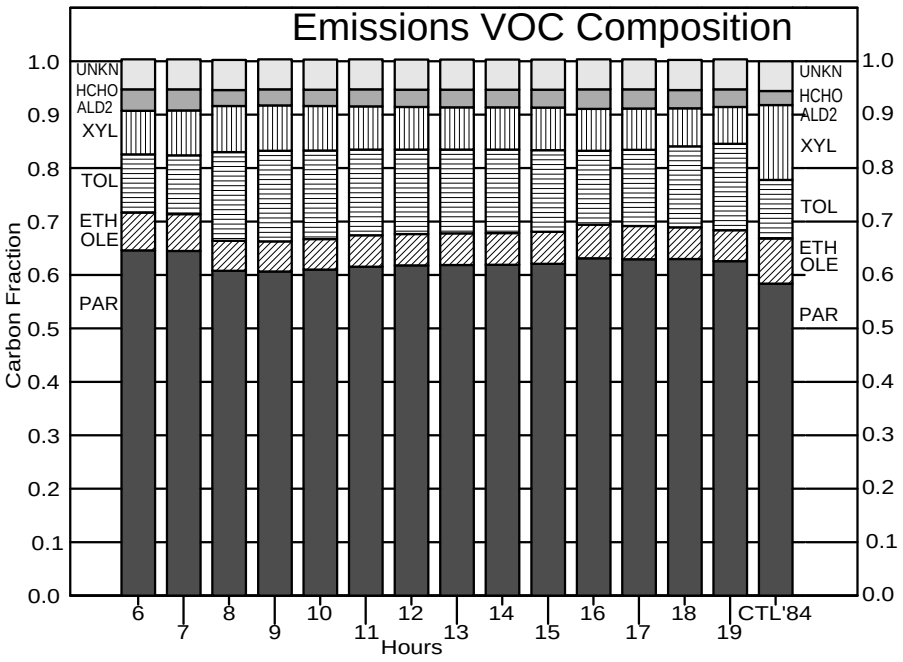

Figure 6:. Model Predicted and Observed VOC composition in 6 × 6 5-km cells near downtown Charlotte NC in 1987 UAM scenario. The bars labeled with hours are the model’s composition, the last bar on right is the average from EPA ambient VOC canister sampling program. Note the difference in toluene and xylene.

NO decrease due to chemistry. Vertical transport of NO_2 removed 34 ppb of NO_2 from layer one. In keeping with the view that this was a relatively stagnant episode, horizontal transport of NO_2 was very low, only -1.6 ppb.

VOCs: In the VOC process plot in Figure 5, we see that total emissions were 344.6 ppbC which combined with the NO_x emissions gives a morning peak emissions VOC-to-NO_x ratio of 5.4:1. The model VOC-to-NO_x ratio based on mixing ratios, however, was 7.7:1, the difference being due to carry-over VOC from the day and night before. Note that the isoprene emissions into the 6 × 6 grid was 37.8 ppbC, yet its contribution to the VOC mixing ratio was almost undetectable. Another time series process analysis not shown here revealed that chemical loss accounted for 70% and that vertical transport accounted for 29% of the isoprene emissions. Note that in the middle of the day, isoprene emissions were about 1/4 of the total VOC emissions. If isoprene is removed from the total VOC emissions, then the anthropogenic-VOC-to-NO_x ratio would be 4.7:1, which is a factor of 1.6 lower than that based on the mixing ratios. This shows some of the difficulty in attempting to compare model predictions with ambient observations and blaming

the differences on the emissions inventory.

Before we leave the issue of VOC emissions, let us illustrate another problem that "process analysis" found in the the UAM inputs. Figure 6 shows a bar chart of VOC composition for each hour in the 1987 Charlotte UAM scenario. At the right end of the chart, we show the average composition that was determined from a 6–9 AM canister sampling program (ambient observations) that was conducted in Charlotte in 1984 as part of a larger EPA program. While there is remarkably good agreement for the classes paraffins, olefins, and aromatics, within the aromatics class there is a large difference: the TOL to XYL ratio in the model is backwards compared to the observations, i.e., the model's TOL was about twice the model's XYL. This disagreement prompted us to conduct a detail examination of TOL-to-XYL ratios in the emissions input files which lead to the discovery that *the speciation for all the area surface coatings and solvents were computed with a single species profile by EPS 2.0,* the EPA-approved UAM emissions processor. Subsequent investigation of this profile revealed that it was based on only *four* paint samples from L.A. that were taken in the late 1970's and these samples were very high in xylene and very low in toluene. EPA's Emissions Inventory Group has been informed of this error and they are now creating new speciation profiles based on newer data.

Ozone: In the O_3 process plot in Figure 5, we see that the early morning source of O_3 was vertical transport from aloft. Chemistry was a negative contributor to O_3 during this time period as the freshly emitted NO titrated the downward mixed O_3. After 0900 LDT, chemistry became a producer of O_3, and remained positive until sunset, producing a total of 113.9 ppb of O_3. After chemistry started to produce O_3, vertical transport out of the layer one cell became a loss process. Deposition of O_3 was a significant loss process, consuming about 38 ppb of O_3. Until 1600 LDT, horizontal transport of O_3 was negligible, but at 1600 LDT in this scenario, horizontal transport brought 29 ppb of O_3 into this 6×6 cell area that already had the highest O_3 mixing ratio in the model. This additional O_3 increased the 6×6 cell's O_3 mixing ratio from 105 ppb to 135 ppb. This was in dramatic contrast to the observed values reported by the two monitors located within the 6×6 cells, which showed decreases of O_3 during this time period (see Fig. 7). While horizontal transport was increasing the cell's mixing ratio, vertical transport was removing less than half the increase and chemical production was still increasing the mixing ratio by about 20 ppb. Individual cells within the 6×6 region showed even more dramatic effects: as much as an 80 ppb increase in O_3

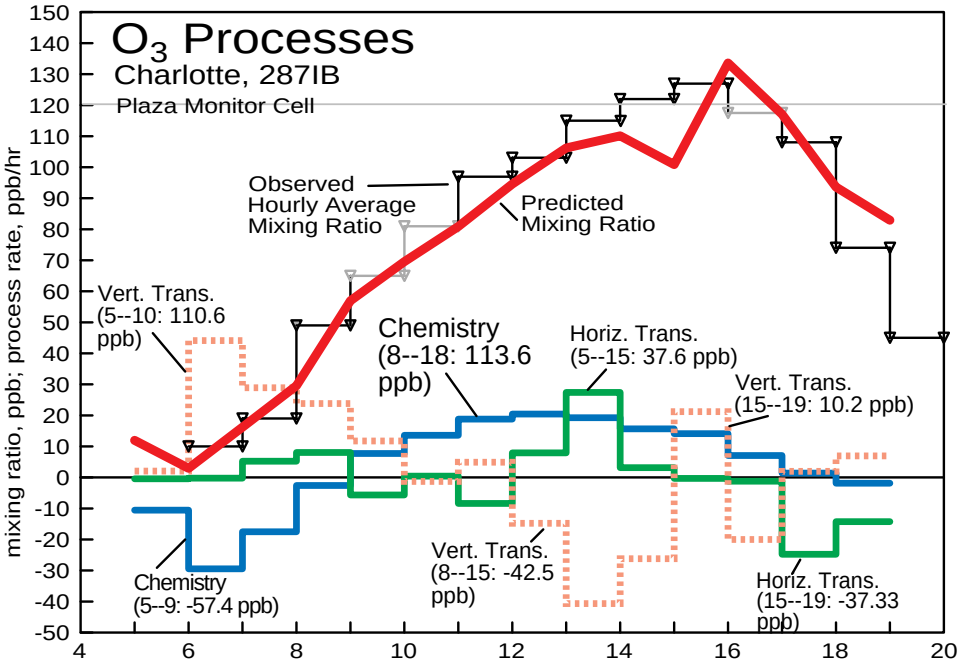

Figure 7: UAM predicted and observed O_3 mixing ratio and the change caused by each process in the UAM.

from 1600 to 1700 LDT producing a peak O_3 mixing ratio of 170 ppb (see Fig. 8).

Because “process analysis” plots made it clear that horizontal transport was responsible for this large increase, the incorrect behavior of the model was traced to problems in the Diagnostic Windfield Model (DWM) producing artificial convergence due to inappropriate interpolation of the hourly monitored wind data. Numerous experiments with the DWM were unable to resolve this problem and it was eventually necessary to use manual “objective analysis” of the wind data to obtain any reasonable predictions.

Other Wind Problems Figure 7 shows a process time series plot for O_3 for a single surface cell (the one containing the Plaza O_3 monitor—the middle cross in Figure 4) and it reveals another problem we have repeatedly observed in UAM simulations: a switch in the direction of vertical transport when there is a major change in wind direction in the UAM. In this plot observe that vertical transport was first positive into the lower layer during the morning hours as the mixing height was rising and O_3 from aloft was being brought down. Once the cell began to produce O_3 chemically, i.e., after 1000 LDT, vertical transport became strongly

negative, carrying the higher concentration O_3 in the lowest cell upward. That is, until the hour 1500–1600 LDT in which *suddenly vertical transport was a source of* O_3 *in the lowest cell.* At 1600 LDT, the vertical transport once again returned to its former nature. This one hour of positive vertical O_3 transport caused a significant "glitch" in the O_3 mixing ratio time series, resulting in the over-prediction and a predicted excedance of the NAAQS for this cell. What happened during the hour starting at 1500? The wind, which in the UAM is held constant for each hour and is only changed on the hour, made a major change in direction at 1500 LDT. Every UAM scenario we have run in which the wind made a large shift in direction in the afternoon has exhibited this vertical transport transient behavior. Because the winds in each layer of UAM are independent of each other, and the model attempts to conserve mass by means of a calibration gas tracer species, the rapid shift in winds from one time step of the model to the next results in an artifact in vertical transport to compensate for the dynamic imbalance in the model.

2.2.3 IPRA Process Composition

Figure 8 shows a "process composition time series" plot for O_3 in a single cell (the one containing the Arrowwood O_3 monitor) in the 287FC UAM simulation for Charlotte, NC. By "process composition" we mean that we have effectively "colored" the O_3 by the type of process that gave rise to the O_3 that is still in the cell at a particular time. At the beginning of the analysis time all the O_3 in the cell would be from the "initial process". As time proceeds and the meteorological processes cause vertical cell growth and horizontal mass flow, this "initial O_3" decreases and O_3 with other process origins are brought into the cell. For example, in the top plot of Fig. 8 we see that vertical transport from layer two into the layer one cell began to increase the cell's O_3 at 0600 LST (at the same time, this decreased the mixing ratio of the "initial O_3" because of dilution). Also at the same time, O_3 that originated somewhere to the west of the Arrowwood cell was being transported into the Arrowwood cell. At 0700 LST, transport also began to contribute O_3 from the north of the Arrowwood cell. We also see from the plot that after 1500 LST, there was a very large amount of O_3 transported from the north and that this was responsible for the large and rapid rise in O_3 from about 100 ppb to over 170 ppb.

These process composition plots are possible because each cell in an Eulerian model is well-mixed, and therefore they can be treated as a continuous stirred tank reactor (CSTR), which is a chemical engineering term for a common type of flow-through reactor. In a CSTR, just as in an Eulerian model cell, mass flows into the reactor volume, mass flows out of the reactor volume, and reactions occur

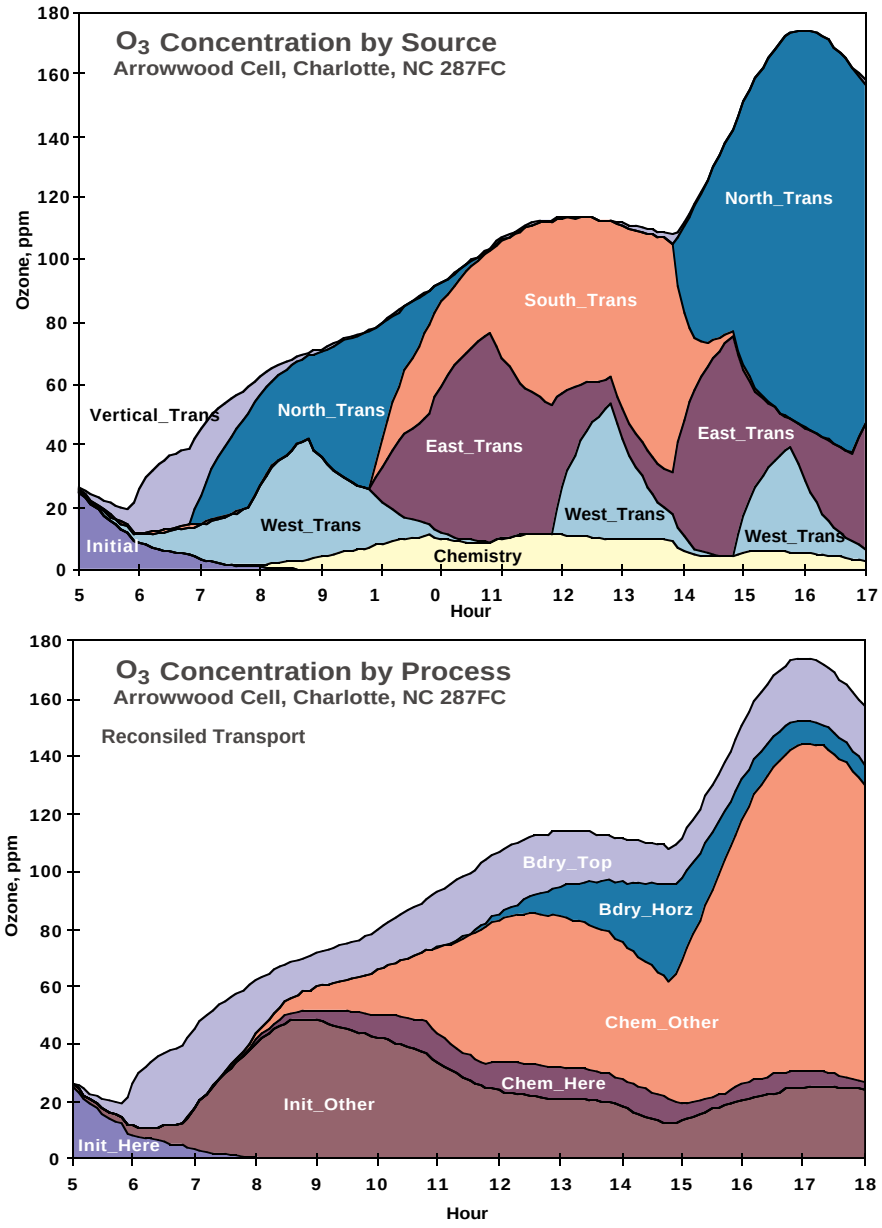

Figure 8:. Process composition times series for O_3 in Episode 287FC Charlotte, NC UAM simulation. TOP: Sources of O_3 by process in Arrowwood Cell; BOTTOM: Sources of O_3 by process in Arrowwood Cell with transport sources replaced by original sources.

in the volume. By performing a mass balance on the cell and using the mass changes by process from the IPR file for the cell as a function of time, we can

develop the fraction of mass in a cell that was accumulated from each source (details of how to carry out these calculations are available in [14]). By keeping such a "process composition" on every cell and by replacing the transported-in mass with the process composition of the up-flow cell, i.e., we resolve the mass of material transported in a cell into its process composition by applying to it the composition of the material in the cell from which the transport is occurring. When such calculations are carried out at each timestep, we can obtain a new "process composition" time series plot that looks like the bottom plot in Fig. 8.

In the bottom plot, there is no mass labeled with transport directions. Instead the original process origins of the transported masses have been identified and these have been collected into groups of origin. For example, "Init_Other" in the plot represents O_3 that was initial O_3 in one of the other 25 by 25 cells at the start of the analysis. "Bdry_Top" represents O_3 that came through the layer one top boundary in any of the 25 by 25 cells and "Bdry_Horizontal" represents O_3 that came from outside the 25 by 25 cells.

This latter plot shows that until after 1200 a large amount of O_3 in this cell came from O_3 that was initially present in the 25 by 25 cell area at the start of the day or from O_3 that was aloft–that is, "old O_3."

In Figures 9 and 10 we take a different view of this same O_3. These "bar" plots show the spatial distribution of the origins of the O_3 that was in the Arrowwood cell at the indicated times. For these plots, only the chemistry process that created the O_3 in the other cells has been visualized. These plots provide the spatial contributions for the two times, 1300 and 1700 LDT. Refer to Fig. 8, and think of two vertical lines at 1300 and at 1700. At these times, chemistry processes had been responsible for 55.6% and 68.6% of the O_3 in Arrowwood's cell. Fig. 9 and 10 show the spatial distribution of these chemical contributions.

This type of analysis can be extremely useful, for example, in determining the extent to which a particular source region, such as a road, would contribute to peak O_3 in selected areas.

2.2.4 IRR Chemical Process Analysis

This type of analysis is applied to the chemical transformations within model cells or aggregated model cells using the IRR data from the chemical reaction mechanism included in the air quality model. Details on how this analysis works are in the literature [1–4]. Basically we have adopted an abstract or systems approach, recognizing two inter-acting cycles (the $\cdot$OH radical cycle and the NO

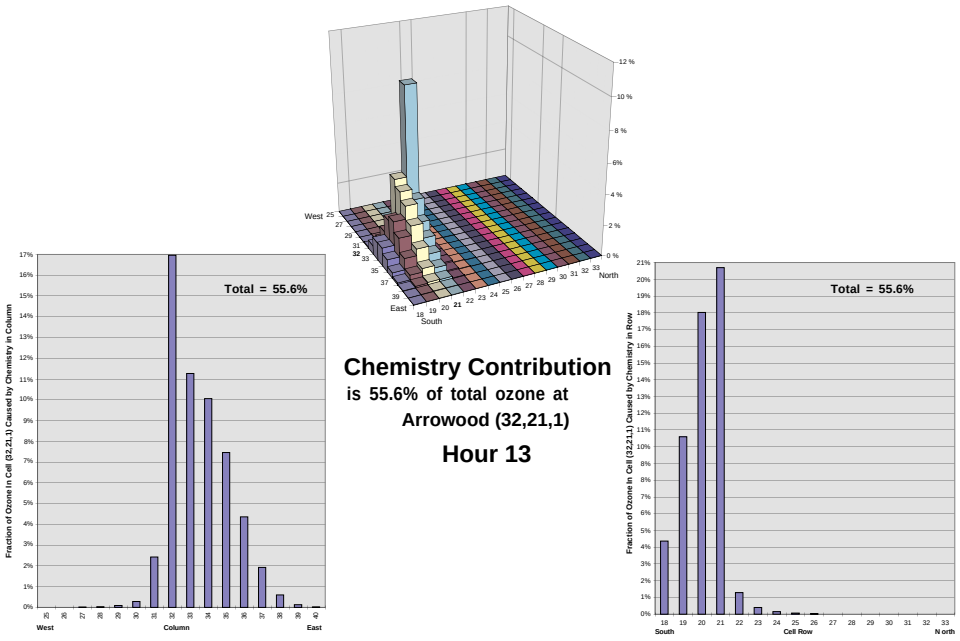

Figure 9:. Process composition spatial contribution to a single cell’s O_3 in Episode 287FC Charlotte, NC UAM simulation. The 3-D plot shows the contribution of just chemistry processes in each cell of a 25 by 25 cell area to Arrowwood cell’s O_3 at 1300 LDT. The 2-D plots show this contribution summed along the rows and columns. At this time, 55.6% of the O_3 in the Arrowwood cell was from chemistry processes that occurred in one of the 25 by 25 cells.

oxidation cycle (see Fig. 11), within a positive feedback loop (the photolysis of O_3 provides about one-half of the new radicals in the system). Radicals are accounted for via initiation, propagation, and termination processes. Oxides of nitrogen are accounted for via emissions, oxidation, and terminal product production. The two cycles are coupled via odd-production by reactions such as

$$HO_2^{\cdot} + NO \longrightarrow NO_2 + {}^{\cdot}OH$$
$$RO_2^{\cdot} + NO \longrightarrow NO_2 + RO^{\cdot}$$

which is necessary for both the radical and nitrogen cycles to continue.

This systems process view introduces several important new parameters that can be used to classify and compare the chemistries of different scenarios for the same model, the same scenario for different models, or different locations, scenarios, and models. Some of these new parameters are:

- “new radical source strength”—new radicals are formed by photolysis of organic (mostly aldheydes) and inorganic (mostly O_3) species that are both present initially and are formed via the oxidation cycles. We have found that for urban simulations, about half of the radicals come from organic and

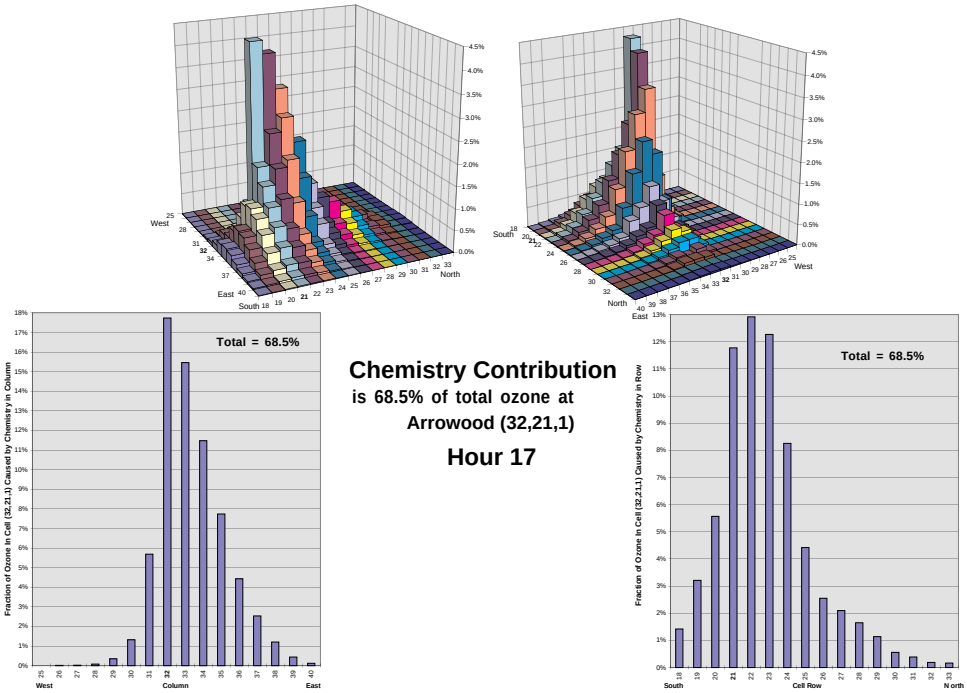

Figure 10:. Process composition spatial contribution to a single cell’s O_3 in Episode 287FC Charlotte, NC UAM simulation. The 3-D plot shows the contribution of just chemistry processes in each cell of a 25 by 25 cell area to Arrowwood cell’s O_3 at 1700 LDT. The 2-D plots show this contribution summed along the rows and columns. At this time, 68.5% of the O_3 in the Arrowwood cell was from chemistry processes that occurred in one of the 25 by 25 cells.

about half come form inoganic sources. That is, O_3 is very important in producing more O_3 (see details in [3]). In Fig. 11 there was 27.9 ppb of new $\cdot OH$ produced. In a cell centered over NY City in a RADM simulation, there was 34.1 ppb new $\cdot OH$ produced.

- “$\cdot OH$ propagation factor” and chain length—each new radical created above is used, re-created, and used again in a chain oxidation process. We measure the fraction of $\cdot OH$ radicals that make it all the way through the chain each cycle and this is called the $\cdot OH$-propagation factor. We have found that this is usually about 0.75 regardless of chemical mechanism, e.g., in the NY City RADM simulation $\mathbf{P}_r$ was 0.747 giving 3.96 cycles per $\cdot OH$. The throughput for the CB4 mechanism in Charlotte translates into 4.11 cycles for each $\cdot OH$ before being lost in termination. The reacted VOC in Charlotte for a 36^2 km area was 128.1 ppbV, where as for NY City for RADM for a 20^2 km area this was 112.9 ppb.
- “NO propagation factor” and chain length—similar to $\cdot OH$-propagation fac-

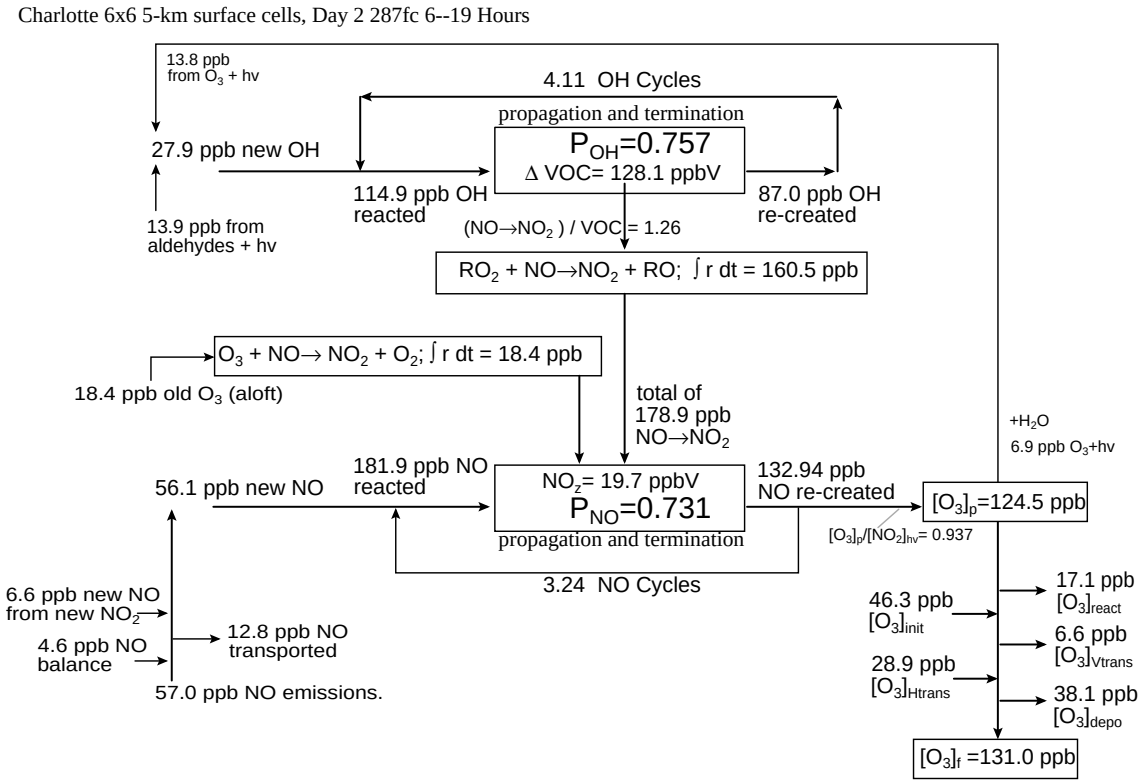

Figure 11:. The ·OH and NO_x Cycles from Integrated Reaction Rates for 6 by 6 Cell Area in UAM Scenario 287FC for Charlotte, NC.

tor, each NO is oxidized to NO_2, and re-created via photolysis to be re-oxidized again. Some reactions remove NO and NO_2 leading to less than 100% throughput. We have found that in most models this factor is about 0.73–0.78, or each NO is used about 3.2 to 4.4 times before being lost. New NO (or NO emissions in the 36^2 km area in Charlotte were 56 ppb for the day, where as in NY City for a 20^2 km area they were 47.9 ppb.

- “NO oxidations per VOC consumed”—this is the total number of NO’s oxidized divided by the total amount of primary VOC reacted and is a measure of the “reactivity” of the VOCs in the model. This value was 1.84 for the RADM mechanism in NY City for fresh VOC emissions, but as shown in Fig. 11 was only 1.26 for CB4 mechanism in Charlotte. This was traced to fact that on this second day of simulation in a stagnant episode, about 1/4 of the reacted VOC was older aged VOC, which has a much shorter oxidation chain length and therefore fewer NO-to-NO_2 conversions per chain.
- “O_3 produced per NO_2 photolysis”—not all of the atomic oxygen that is

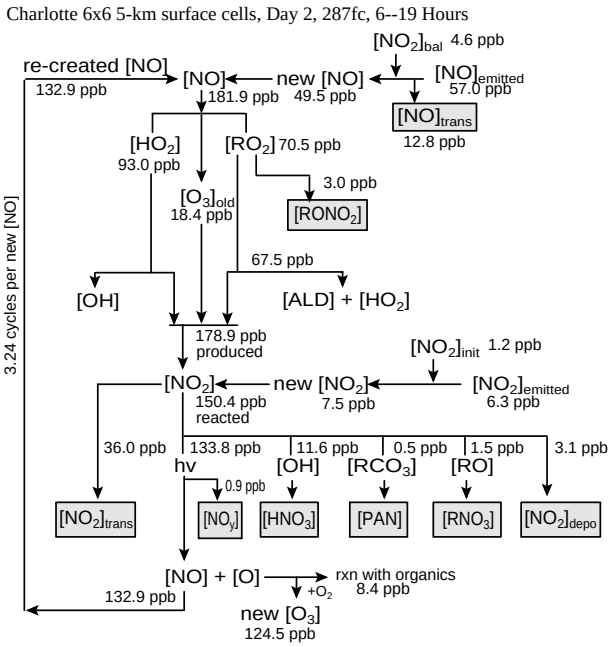

Figure 12:. The NO Cycle and Mass Balance from Integrated Reaction Rates for 6 by 6 Cell Area in UAM Scenario 287FC for Charlotte, NC.

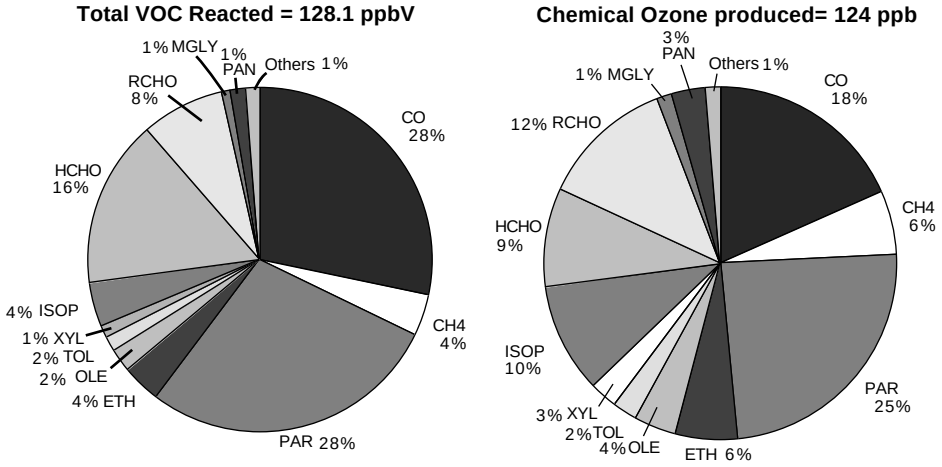

Figure 13:. The amount of VOC reacted and O_3 formed by reaction of each VOC for 6 by 6 Cell Area in UAM Scenario 287FC for Charlotte, NC.

produced when NO_2 photolyzes is converted into O_3. In the NY City RADM simulation this fraction was 0.909 compared to 0.937 in the UAM Charlotte simulation.

From this brief comparison of IRR process parameters we can see that the

Table 3:. NO_y Mass Balance from Integrated Reaction Rates for 6 by 6 Cell Area in UAM Scenario 287FC for Charlotte, NC. Units are parts per billion (ppbN). These results show a 4.8 ppb gain in NO_y mass over the course of the simulation. The error does not arise in the chemistry solver, but must be due to errors in the transport solver.

Process	NO		NO_2		NO_y - NO_x		NO_y		*Sum*
	Sources	*Sinks*	*Sources*	*Sinks*	*Sources*	*Sinks*	*Sources*	*Sinks*	
Initial Conc.	0.93		8.97		7.18		17.08	0.00	17.08
Emissions	57.01		6.28		0.00		63.29	0.00	63.29
Net Horizontal Trans		-0.63		-1.66	1.44		1.44	-2.28	-0.84
Net Vertical Trans		-12.17		-34.36	2.86		2.86	-46.53	-43.68
Chemistry	132.94	-182.48	185.08	-147.32	19.21	-7.44	337.23	-337.23	0.00
Deposition		-0.06		-3.12		-13.59	0.00	-16.77	-16.77
Final Conc		-0.11		-5.27		-9.31	0.00	-14.69	-14.69
Totals	190.87	-195.44	200.34	-191.73	30.68	-30.34	421.90	-417.51	4.39
Source-Sink	-4.57		8.61		0.35		4.39		4.39

downtown area of Charlotte, NC has chemistry just as intense as the center of NY City. A major difference, however, is that Charlotte only has only one area with this intensity, whereas the next area downwind in NY City was similar to the one described here and the one after that too. Thus, in Charlotte chemical processes decrease rapidly with distance from the center city, whereas in NY City these same processes are sustained at high levels over a much larger distance.

Fig. 13 shows another type of output that can be produced by IRR/MB analysis. We have developed a set of history lists that are maintained on each reaction. Using these, we can “replace” intermediates that are formed as products in the reaction of the primary VOCs with the products of the reactions of the intermediates, thus eliminating the intermediate species. In this way we can obtain an accurate assessment of the contribution of each primary VOC to the total O_3 production as is shown in the figure. In every case where we have performed this analysis, CO, methane, and the paraffins—*the least reactive species*—have accounted for more than half the O_3 produced. This is due to large mass in the urban area, whereas the so-called most reactive species have small emitted masses and are rapidly consumed before producing much O_3. The radicals produced by these so-called reactive species are what really do the work using the large mass of CO, methane, and paraffins.

Finally, Table 3 shows a disturbing result of a full mass balance for NO_y for this case. The total NO_y sources plus initial NO_y *exceed* the total NO_y sinks plus final NO_y by 4.8 ppb. We had expected the chemistry solver in UAM, which uses steady-state approximations, to be at fault, but to our surprise the chemistry process was balanced within 0.005 ppbN and instead the problem lies somewhere within the

transport processes. A similar problem showed up in a St. Louis UAM simulation. EPA has given SAI, the UAM authors, a task order to investigate this problem.

3 IPRA Summary

Our work in the last few years has resulted in the development of a powerful collection of model analysis tools, which have significantly advanced our understanding of the dynamic interaction among emissions, transport, and chemical transformations. These tools have been enthusiastically received by the modeling and policy making community.

Our problem now is to improve the operation of the tools and to make them more generally available. In addition, the number of cases for which the tools have been applied is limited and yet we have learned a large amount about the operation of the Eulerian models and the interactions of chemistry and meteorology We have also found errors and model formulation problems. We therefore need to conduct analyses with these tools on a wide variety of scenarios covering a large range of conditions.

Base URL in the references is
`airsite.unc.edu/pdfs/ese_unc/jeffries/`.

References

[1] Jeffries, H. E., "Photochemical Air Pollution," Chapter 9 in *Composition, Chemistry, and Climate of the Atmosphere,* Ed. H.B. Singh, Van Nostand-Reinhold, New York, 1995.

[2] Jeffries, H. E., "A Different View of Ozone Formation", Fuel Reformulation, 3(1): 57; ISSN: 1062-3744,1993. "ftp://Base_URL/ipradocs/fuelrefm.pdf"}

[3] Tonnesen, S., Jeffries, H.E., "Inhibition of Odd Oxygen Production in Carbon Bond IV and Generic Reaction Set Mechanisms," *Atmos. Environ*,**28**:(7) 1339–1349, 1994.

[4] Jeffries, H.E., Tonnesen, S., "A Comparison of Two Photochemical Reaction Mechanisms Using a Mass Balance Process Analysis," *Atmos. Environ.,* **28**(18):2991–3003, 1994.

[5] Tonnesen, S., Jeffries, H.E., "The Contribution of Biogenic Hydrocarbons, Carbon Monoxide, Methane, and VOCs to Ozone Production in 39 Urban Areas," "ftp://Base_URL/ipradocs/39cities.pdf"}.

[6] Tonnesen, S., Jeffries, H.E., "Analysis of Uncertainty in the Use of Incremental Reactivity for Hydrocarbon Reactivity Adjustment Factors," "ftp://Base_URL/ipradocs/increact.pdf"}

[7] Jang, J.C., Jeffries, H. E., Byun, D., Pleim, J.E., "Sensitivity of Ozone to Model Grid Resolution: Part I. Application of High-Resolution Regional Acid Deposition Model," *Atmos. Environ.*, **29**(21):3085, 1995..

[8] Jang, J.C., Jeffries, H. E., Tonnesen, S., "Sensitivity of Ozone to Model Grid Resolution: Part II. Detailed Process Analysis for Ozone Chemistry," *Atmos. Environ.,* **29**(21):3114, 1995.

[9] Lo, Chao-Yang Sunny and Jeffries, H.E., "A Quantitative Technique for Assessing Pollutant Source Location and Process Composition in Photochemical Grid Models," presented at the National AWMA conference, Toronto, Ontario, Canada, 1997, "ftp://Base_URL/ipradocs/pca_awma.pdf"}.

[10] Wang, Z., Langstaff, J., Jeffries, H.E., "Application of Integrated Process Analysis to Investigate Urban Airshed Model Sensitivity to Speciation in VOC Emissions Data," presented at the National AWMA conference, San Antonio, TX, 1995.

[11] Jeffries, H.E., "Process Analysis For UAM Episode 287," memo to Brock Nicholson, NC-DEHNR, April,8 1994, "ftp://Base_URL/ipradocs/panal287.pdf"}.

[12] Jeffries, H.E., Keating, T., Wang, Z., "Integrated Process Rate Analysis of the Impact of NOx Emission Height on UAM-modeled Peak Ozone Levels", Final Topical Report, prepared for the Gas Research Institute, Chicago, IL, 1996,
also at "ftp://Base_URL/ipradocs/uncgri1.pdf"}and "ftp://Base_URL/ipradocs/uncgri2.pdf"}

[13] Wang, Z. "Summary of Modifications Made to the Regulatory Version of the Urban Airshed Model to Include IPRA Output," UNC Environemental Modeling Laboratory Technical Note, 1995.

[14] Jeffries, H.E., "How to Track Origins of NO_y Mass in Eulerian Models", UNC Environmental Modeling Laboratory Technical Report, 1993 (available).